Supplemental Materials

A partial reconstitution implicates DltD in catalyzing lipoteichoic acid D-alanylation

B. McKay Wood, John Santa Maria, Leigh Matano, Christopher Vickery, Suzanne Walker

Contents:

Table S1. Summary of phenotypes used to study the DLT pathway

	Bacillus subtilis	*Staph. aureus*	*Strep. gordonii*	*Strep. mutans*	*Strep. agalactiae*	*Strep. pneumoniae*	*Group A Strep.*	*Group B Strep.*	*Lactobacillus rhamnosus*	*Lactobacillus reuteri*	*Lactobacillus casei*	*Lactococcus lactis*	*Clostridium difficile*	*Listeria monocyt.*	*Enterococcus facaelis*
cell wall D-ala content	(1)	(2)	(3)	(4) (5)		(6)	(7)		(8)				(9)		(10)
cell surface Western			(3)												
Antibiotic resistance															
CAMPs resistance		(2) (11) (12) (13) (14)		(15) (5)	(16)	(6)	(7)	(17)	(18)	(19)	(20)		(9)	(21)	(10)
daptomycin		(14) (22) (23) (24) (25)													
methicillin	(26)	(11) (27)													
definsin		(2) (25)			(16)				(18)						
tunicamycin		(28) (29)													
cationic lipodepsipeptides	(30)														
cationic phospholipase A2		(31)													
skin extracts		(13)													
lysostaphin and lysozyme	(32)	(11) (33)													
anionic detergent									(18)						
Growth and homeostasis															
autolysis	(34) (26)	(27)					(7)		(18)	(19)		(35)			
low pH growth		(36) (37)		(4)			(7)		(18)	(19)	(20) (38)				
motility defect	(1)														
cell length									(18)						
coaggregation			(3)												
protein secretion	(40)														
Mg2+ induction		(36) (41)													
colony spreading		(42)													
growth medium [salt]		(43)													
high growth temperature											(20)				
Pathogenesis															
virulence		(44)			(16)									(21)	
neutrophil evasion		(44)			(16)		(7)								
adherence							(7)							(21)	(10) (45)
biofilm formation		(39)								(19)					(10)
mouse colonization										(19)					
human T-cell activation		(46)													
Cell surface charge															
cytochrome c	(26)	(2) (23)		(5)			(7)								
crystal violet				(5)											
GFP		(2)													
Cell membrane fluidity															
fluorescence polarization		(23)													

Table S1. Primers

Primer	Sequence 5' to 3'	Description
	Cloning	
PMW56	GCCGCGCGGCAGCCATACAGATATTATTAACAAGCTGC	Infusion forward cloning primer for dltA minus start codon into pET15b-NdeI/BamHI
PMW57	GTTAGCAGCCGGATCCTTATCCGTTAATTACCTCTGCAATTTTC	Infusion reverse cloning primer for dltA into pET15b-NdeI/BamHI
PMW14	TTTCATATGGAATTTAGAGAACAAGT	dltC cloning forward primer with TTT-NheI addition to 5’
PMW8	TTTGGATCCTCATCGTAACTCTTCTAATGC	dltC cloning reverse primer with TTT-BamHI addition to 3’-end of gene, reverse complement
PMW60	GCCGCGCGGCAGCCATAAATTAAAACCTTTTTTACCC	Infusion forward cloning primer for dltD minus start codon into pET15b-NdeI/BamHI
PMW61	GTTAGCAGCCGGATCCTTAATTTTTAGGTTTATCTACTTC	Infusion reverse cloning primer for dltD into pET15b-NdeI/BamHI
PMW62	GCCGCGCGGCAGCCATACAGGATTAGTAAATGAAAAGAC	Infusion forward cloning primer for dltDtrunc into pET15b-NdeI/BamHI
PMW63	GCCGCGCGGCAGCCATGCAATATTAGGTTTAGGCACG	Infusion forward cloning primer for Ecoli acpS minus start codon into pET15b-NdeI/BamHI
PMW64	GTTAGCAGCCGGATCCTTAACTTTCAATAATTACCGTGGC	Infusion reverse cloning primer for Ecoli acpS into pET15b-NdeI/BamHI
SM61	GATTGTCGACTGAGTTCTAATGAGGGAG	SalI forward primer for cloning SaDLT into pLOW
SM64	TTAAGGATCCTTAATTTTTAGGTTTATCTACTTC	BamHI reverse primer for cloning SaDLT into pLOW
SM148	GATTGGTACCTGAGTTCTAATGAGGGAG	KpnI forward primer for cloning dltABCD plus RBS into pTP63-KpnI/BlpI
SM149	TTAAGCTCAGCTTAATTTTTAGGTTTATCTACTTC	BlpI reverse primer for cloning dltABCD plus RBS into pTP63-KpnI/BlpI
PMW142	CAAAAATTAATTTCAGAAGAAGATTTATTAAAACCTTTTTTACCCATTTTAATTAGTGG	5’-dltD myc-tagging forward primer
PMW143	TAAATCTTCTTCTGAAATTAATTTTTGTTCTTTCATCGTAACTCTTCTAATGC	5’-dltD myc-tagging reverse primer
PMW144	TTAAGCTCAGCTAAATCTTCTTCTGAAATTAATTTTTGTTCTTAATTTTTAGGTTTATCTACTTCAGG	3’-dltD myc-tagging reverse primer
PMW181	TTTGGTACCTGAGTTCTAATGAGGGAGACTTAATATGAAATTAAAACCTTTTTTACCC	dltD cloning forward primer with KpnI site + SaDLT RBS addition to 5’-end (used with SM149)
PMW214	AGAATCATGGAACAAAAATTAATTTCAGAAGAAGATTTAAGTTCACAAAAAAAGAAAATT	LtaS N-terminal myc-tagging forward primer to be used with PMW216 in the construction of the insert for cloning into pTP63 (to be followed by amplification with PMW215)
PMW215	AGAGTATGATGGTACCTATCTAAATAACGGGGGAAAGAATCATGGAACAAAAATT	Infusion forward cloning primer for ltaS with native RBS and N-terminal myc tag into (KpnI/BlpI) pTP63
PMW216	AGCGACCGGCGCTCAGCTTATTTTTTAGAGTTTGCTTTAGG	Infusion reverse cloning primer for ltaS into (KpnI/BlpI) pTP63
PMW217	AGAGTATGATGGTACCTATCTAAATAACGGGGGAAAGAATCATGAGTTCACAAAAAAAGA	Infusion forward cloning primer for ltaS with native RBS into (KpnI/BlpI) pTP63
PMW218	CTTCTTCTGAAATTAATTTTTGTTCTTTTTTAGAGTTTGCTTTAGG	LtaS C-terminal myc-tagging primer (stop codon removed) to be used with PMW217 in the construction of the insert for cloning into pTP63 (to be followed by amplification with PMW219)
PMW219	AGCGACCGGCGCTCAGCTTATAAATCTTCTTCTGAAATTAATTTTTG	Infusion reverse cloning primer for ltaS with C-terminal myc tag (new stop codon) into (KpnI/BlpI) pTP63 (to be used with product of PMW217/218)

Sequencing		
PMW97	CGACTGAAGTTACGGACAATGC	Forward sequencing primer for the 3’-end of dltA and the 5’-end of dltB
PMW126	GTGTCTAACAGCAATGCTTTGTGG	Reverse primer for SaDLT promoter sequencing; anneals inside dltA near the 5' end
PMW149	GTAGATAATGGTGGTAAAATTTACG	Forward sequencing primer dlt downstream region (from within dltD)
PMW156	CAATCAAAATCGTTGAGTTATGTGC	Reverse primer for amplifying from downstream of dltD on the S. aureus chromosome
DltD mutagenesis		
PMW129	GTATTATCCTATATACGGCTCTGCTGAATTAGGTAAAGATGACCC	dltD S70A mutagenesis forward primer
PMW130	GGGTCATCTTTACCTAATTCAGCAGAGCCGTATATAGGATAATAC	dltD S70A mutagenesis reverse primer
PMW150	GTATTATCCTATATACGGCTCTGTTGAATTAGGTAAAGATGACCC	dltD S70V mutagenesis forward primer
PMW151	GGGTCATCTTTACCTAATTCAACAGAGCCGTATATAGGATAATAC	dltD S70V mutagenesis reverse primer
PMW204	GTATTATCCTATATACGGCTCTTGTGAATTAGGTAAAGATGACCC	dltD S70C mutagenesis forward primer
PMW205	GGGTCATCTTTACCTAATTCACAAGAGCCGTATATAGGATAATAC	dltD S70C mutagenesis reverse primer
PMW222	TATCCTATATACGGCTCTAGTGCTTTAGGTAAAGATGACCCATTTAATCC	dltD E71A mutagenesis forward primer
PMW223	GGATTAAATGGGTCATCTTTACCTAAAGCACTAGAGCCGTATATAGGATA	dltD E71A mutagenesis reverse primer
PMW224	TATCCTATATACGGCTCTAGTCAATTAGGTAAAGATGACCCATTTAATCC	dltD E71Q mutagenesis forward primer
PMW225	GGATTAAATGGGTCATCTTTACCTAATTGACTAGAGCCGTATATAGGATA	dltD E71Q mutagenesis reverse primer
PMW230	CAAGTATTATCCTATATACGGCTCTAGTAATTTAGGTAAAGATGACCCATTTAATCC	dltD E71N mutagenesis forward primer
PMW231	GGATTAAATGGGTCATCTTTACCTAAATTACTAGAGCCGTATATAGGATAATACTTG	dltD E71N mutagenesis reverse primer
PMW131	TAACATTTATTATTTCACCAGCATGGTTTACAAACCATGG	dltD Q129A mutagenesis forward primer
PMW132	CCATGGTTTGTAAACCATGCTGGTGAAATAATAAATGTTA	dltD Q129A mutagenesis reverse primer
PMW206	TAACATTTATTATTTCACCATGTTGGTTTACAAACCATGG	dltD Q129C mutagenesis forward primer
PMW207	CCATGGTTTGTAAACCAACATGGTGAAATAATAAATGTTA	dltD Q129C mutagenesis reverse primer
PMW133	CATTTATTATTTCACCACAAGCATTTACAAACCATGGTTTAACG	dltD W130A mutagenesis forward primer
PMW134	CGTTAAACCATGGTTTGTAAATGCTTGTGGTGAAATAATAAATG	dltD W130A mutagenesis reverse primer
PMW208	CATTTATTATTTCACCACAATGTTTTACAAACCATGGTTTAACG	dltD W130C mutagenesis forward primer
PMW209	CGTTAAACCATGGTTTGTAAAACATTGTGGTGAAATAATAAATG	dltD W130C mutagenesis reverse primer
PMW135	GATTATGAAAAATATGTTATCAGTGCTGCCGTACACATCGGTTGG	dltD D358A mutagenesis forward primer
PMW136	CCAACCGATGTGTACGGCAGCACTGATAACATATTTTTCATAATC	dltD D358A mutagenesis reverse primer
PMW210	GATTATGAAAAATATGTTATCAGTTGTGCCGTACACATCGGTTGG	dltD D358C mutagenesis forward primer
PMW211	CCAACCGATGTGTACGGCACAACTGATAACATATTTTTCATAATC	dltD D358C mutagenesis reverse primer
PMW137	TATGTTATCAGTGATGCCGTAGCAATCGGTTGGAAAGGTTGGG	dltD H361A mutagenesis forward primer
PMW138	CCCAACCTTTCCAACCGATTGCTACGGCATCACTGATAACATA	dltD H361A mutagenesis reverse primer

DltB mutagenesis		
PMW98	GACATTATCATTCTGGTTCAGAGATTCTATTTACATGAGATCTTTATTCTACATG	dltB C304S mutagenesis forward primer
PMW99	CATGTAGAATAAAGATCTCATGTAAATAGAATCTCTGAACCAGAATGATAATGTC	dltB C304S mutagenesis reverse primer
PMW145	TATTAAAGATTTCTGGAATAGATGG<u>GCT</u>ATGACATTATCATTCTGGTTCAGAG	dltB H294A mutagenesis forward primer
PMW146	CTCTGAACCAGAATGATAATGTCAT<u>AGC</u>CCATCTATTCCAGAAATCTTTAATA	dltB H294A mutagenesis reverse primer
PMW147	TATTAAAGATTTCTGGAATAGATGG<u>AAT</u>ATGACATTATCATTCTGGTTCAGAG	dltB H294N mutagenesis forward primer
PMW148	CTCTGAACCAGAATGATAATGTCAT<u>ATT</u>CCATCTATTCCAGAAATCTTTAATA	dltB H294N mutagenesis reverse primer
PMW73	CATAATGGGAATTTGGGCGGGTATCGAAGTGTAT	dltB H341A mutagenesis forward primer
PMW74	ATACACTTCGATACCCGCCCAAATTCCCATTATG	dltB H341A mutagenesis reverse primer
LtaS mutagenesis		
CRV55	AGCACCTGAAGATGACTTAACAAAAGTATTAA	ltaS S218P mutagenesis forward primer
CRV56	TTCAGGTGCTAGCGCTTTTTGTTGATTATT	ltaS S218P mutagenesis reverse primer
rtPCR		
PMW154	GATTCTTTCCAAACAGTTGGATT	dltC rtPCR primer1 (133nt product)
PMW155	CGTAACTCTTCTAATGCTTCAACG	dltC rtPCR primer2 (133nt product)
PMW240	GAAATCTAAAAGTAAACAGCCACCT	Forward primer to test dltX dltA cotranscription
PMW241	TTACTACCTTGTAATCGATGTGCT	Reverse primer to test dltX dltA cotranscription
PMW242	GACAACCAATTACTATGTTGAATCT	Forward primer to test SAOUHSC_00867 dltX cotranscription (can be used with PMW241 to test dltA cotranscription)
PMW243	GAAGTTATTGTGTGTGTCGCC	Reverse primer to test SAOUHSC_00867 dltX cotranscription

Table S2. Plasmids

Name	Description	Purpose
		E. coli plasmids
pMW16	pET15b-dltA1	N-terminal hexahistidine tagged SaDltA expression vector for T7 infected E. coli
pMW18	pET15b-dltD1	N-terminal hexahistidine tagged SaDltD expression vector for T7 infected E. coli
pMW19	pET15b-dltDtrunc1	N-terminal hexahistidine tagged N-terminally truncated, soluble SaDltD expression vector for T7 infected E. coli
pMW20	pET15b-dltC2	N-terminal hexahistidine tagged SaDltC expression vector for T7 infected E. coli
pMW21	pET15b-acpS2	N-terminal hexahistidine tagged EcAcpS expression vector for T7 infected E. coli; acpS used to make holo-DltC
pMW138	pET15b-dltD S70A1	Expression plasmid for N-terminally 6His-tagged DltD S70A site-directed mutant (start - 770bp verified)
pMW162	pET15b-dltD E71A2	Expression plasmid for N-terminally 6His-tagged DltD E71A site-directed mutant (1-740bp verified)
pMW164	pET15b-dltD E71N1	Expression plasmid for N-terminally 6His-tagged DltD E71N site-directed mutant; (1-968bp verified)
pMW163	pET15b-dltD E71Q1	Expression plasmid for N-terminally 6His-tagged DltD E71A site-directed mutant (1-740bp verified)
pMW149	pET15b-dltD Q129A1	Expression plasmid for N-terminally 6His-tagged DltD Q129A site-directed mutant (54 - 1119bp verified)
pMW150	pET15b-dltD Q129C1	Expression plasmid for N-terminally 6His-tagged DltD Q129C site-directed mutant (54 - 1119bp verified)
pMW151	pET15b-dltD W130A1	Expression plasmid for N-terminally 6His-tagged DltD W130A site-directed mutant (54 - 1119bp verified)
pMW152	pET15b-dltD W130C1	Expression plasmid for N-terminally 6His-tagged DltD W130C site-directed mutant (54 - 1119bp verified)
pMW134	pET15b-dltD D358A	Expression plasmid for N-terminally 6His-tagged DltD D358A site-directed mutant; sequenced 3/17/2016
pMW139	pET15b-dltD H361A1	Expression plasmid for N-terminally 6His-tagged DltD H361A site-directed mutant (247 - 1165bp verified)
		S. aureus plasmids
pMW35	pLOW-SadltABCD	made by Samir; dlt knockout complementation plasmid;
pMW38	pLOW-SaDLT (dltB H341A)2	S. aureus dlt complementation vector with H341A site-directed mutation; Quikchange colony 2
pMW55	pTP63-SaDLT [2]	Samir's complementation plasmid expressing S. aureus DLT operon; sequenced 5/29/15 and 6/1/15 (verified entire dlt operon except dltA 1-31 and 70)
pMW98	pTP63-dltD1	S. aureus dltD complementation vector (bp 93-1131 verified)
pMW84	pTP63-SaDLT (myc-dltD)1	S. aureus dlt complementation vector with N-terminal myc-tagged dltD; sequenced DltCD genes 7/15/2015
pMW78	pTP63-SaDLT (dltD-myc)2	S. aureus dlt complementation vector with C-terminal myc-tagged dltD (dltD 270-3'end verified)
pMW117	pTP63-SaDLT (myc-dltD S70A)1	S. aureus dlt complementation vector with N-terminally myc-tagged dltD containing S70A site-directed mutation, sequenced 2/8/2016
pMW144	pTP63-SaDLT (myc-dltD S70C)1	S. aureus dlt complementation vector with N-terminally myc-tagged dltD containing S70C site-directed mutation (dltD sequence verified 92-768bp)

pMW121	pTP63-SaDLT (myc-dltD S70V)1	S. aureus dlt complementation vector with N-terminally myc-tagged dltD containing S70V site-directed mutation, sequenced 2/8/2016
pMW160	pTP63-SaDLT (myc-dltD E71A)1	S. aureus dlt complementation vector with N-terminally myc-tagged dltD E71A mutant; sequenced 11/9/2016
pMW167	pTP63-SaDLT (myc-dltD E71N)1	S. aureus dlt complementation vector with N-terminally myc-tagged dltD E71N mutant (29-1015bp of dltD verified)
pMW161	pTP63-SaDLT (myc-dltD E71Q)1	S. aureus dlt complementation vector with N-terminally myc-tagged dltD E71Q mutant; sequenced 11/9/2016
pMW148	pTP63-SaDLT (myc-dltD Q129A)1	S. aureus dlt complementation vector with N-terminally myc-tagged dltD containing Q129A site-directed mutation (dltC verified from 95-3'-end; dltD verified 5'myc tag-1117bp)
pMW145	pTP63-SaDLT (myc-dltD Q129C)1	S. aureus dlt complementation vector with N-terminally myc-tagged dltD containing Q129C site-directed mutation (dltD sequence verified 92-942bp)
pMW124	pTP63-SaDLT (myc-dltD W130A)1	S. aureus dlt complementation vector with N-terminally myc-tagged dltD containing W130A site-directed mutation, sequenced 2/25/2016
pMW146	pTP63-SaDLT (myc-dltD W130C)1	S. aureus dlt complementation vector with N-terminally myc-tagged dltD containing W130C site-directed mutation (dltD sequence verified 82-834bp)
pMW85	pTP63-SaDLT (myc-dltD D358A)1	S. aureus dlt complementation vector with N-terminal myc-tagged dltD D358A site-directed mutant (dltD 191-1131 verified)
pMW147	pTP63-SaDLT (myc-dltD D358C)1	S. aureus dlt complementation vector with N-terminally myc-tagged dltD containing D358C site-directed mutation (dltD sequence verified 531-1080bp)
pMW87	pTP63-SaDLT (myc-dltD H361A)1	S. aureus dlt complementation vector with N-terminal myc-tagged dltD H361A site-directed mutant (dltD 215-1132 verified)
pMW73	pTP63-myc-DltB	S. aureus dlt complementation vector with N-terminal myc-tagged dltB (dltA 1343-3'end and dltB 5'end-696 verified)
pMW75	pTP63-dltB-myc	S. aureus dlt complementation vector with C-terminal myc-tagged dltB (dltB 432-3'end verified)
pMW91	pTP63-SaDLT (dltB-myc H294A)1	S. aureus dlt complementation vector with C-terminal myc-tagged dltB H294A site-directed mutant (dltB 215-1170 verified)
pMW93	pTP63-SaDLT (dltB-myc H294N)1	S. aureus dlt complementation vector with C-terminal myc-tagged dltB H294N site-directed mutant (dltB 189-1161 verified)
pMW95	pTP63-SaDLT (dltB-myc H341A)1	S. aureus dlt complementation vector with C-terminal myc-tagged dltB H341A site-directed mutant (dltB 229-1170 verified)
pMW154	pTP63-myc-ltaS1	S. aureus dlt complementation vector with N-terminally myc-tagged ltaS (verified start-882bp and 1058-1889bp)
pMW156	pTP63-ltaS-myc1	S. aureus dlt complementation vector with C-terminally myc-tagged ltaS (verified 38-725bp and 970-last bp)
pMW165	pTP63-myc-ltaS S218P2	S. aureus integrative vector with N-terminally myc-tagged LtaS and S219P mutation (1-938bp verified)
pMW166	pTP63-ltaS-myc S218P1	S. aureus integrative vector with C-terminally myc-tagged LtaS and S219P mutation (26-938bp verified)

Table S3. Strains

Strain	Background	Genotype/ plasmid	Antibiotic (µg/mL)
		S. aureus	
	RN4220		
	Newman		
JSM1	Newman	ΔdltA	
LM1	Newman	dltB::kanR	Kan(50) Neo(50)
LM2	Newman	dltC::kanR	Kan(50) Neo(50)
JSM2	Newman	dltD::kanR	Kan(50) Neo(50)
	RN4220	auxillary plasmid for integration of pTP63	Tet(5)
	HG003	spa::tn-ErmR	Erm(5)
	SEJ1		
4S5	SEJ1	ΔltaS ΔgdpP	
BMW57	Newman	pLOW	Erm(5)
BMW63	Newman	pMW35 1	Erm(5)
BMW72	Newman	ΔdltA/ pLOW1	Erm(5)
BMW92	Newman	ΔdltA/ pLOW-SaDLT1	Erm(5)
BMW74	Newman	dltB::kanR/ pLOW1	Erm(5) Kan(50) Neo(50)
BMW67	Newman	dltB::kanR/ pLOW-SaDLT1	Erm(5) Kan(50) Neo(50)
BMW90	Newman	dltC::kanR/ pLOW1	Erm(5) Kan(50) Neo(50)
BMW68	Newman	dltC::kanR/ pLOW-SaDLT1	Erm(5) Kan(50) Neo(50)
BMW65	Newman	dltD::kanR/ pLOW	Erm(5) Kan(50) Neo(50)
BMW70	Newman	dltD::kanR/ pLOW-SaDLT1	Erm(5) Kan(50) Neo(50)
BMW173	Newman	pTP63	Cam(10)
BMW174	Newman	pMW84; pTP63-SaDLT (myc-dltD)1	Cam(10)
BMW188	Newman	dltD::kan/ pTP63	Cam(10) Kan(50) Neo(50)
BMW175	Newman	dltD::kan/ pMW84; pTP63-SaDLT (myc-dltD)1	Cam(10) Kan(50) Neo(50)
BMW304	Newman	pMW117; pTP63-SaDLT (myc-dltD S70A)1	Cam(10)
BMW305	Newman	dltD::kan/ pMW117; pTP63-SaDLT (myc-dltD S70A)1	Cam(10) Kan(50) Neo(50)
BMW306	Newman	pMW121; pTP63-SaDLT (myc-dltD S70V)1	Cam(10)
BMW307	Newman	dltD::kan/ pMW121; pTP63-SaDLT (myc-dltD S70V)1	Cam(10) Kan(50) Neo(50)
BMW245	Newman	pMW85; pTP63-SaDLT (myc-dltD D358A)1	Cam(10)
BMW248	Newman	dltD::kan/pMW85; pTP63-SaDLT (myc-dltD D358A)1	TSB/10Cam/50Kan/50Neo
BMW244	Newman	pMW87; pTP63-SaDLT (myc-dltD H361A)1	TSB/10Cm
BMW247	Newman	dltD::kan/pMW87; pTP63-SaDLT (myc-dltD H361A)1	TSB/10Cam/50Kan/50Neo
BMW365	Newman	pMW148; pTP63-SaDLT (myc-dltD Q129A)1	Cam(10)
BMW366	Newman	dltD::kan/ pMW148; pTP63-SaDLT (myc-dltD Q129A)1	Cam(10) Kan(50) Neo(50)
BMW367	Newman	pMW124; pTP63-SaDLT (myc-dltD W130A)1	Cam(10)
BMW368	Newman	dltD::kan/ pMW124; pTP63-SaDLT (myc-dltD W130A)1	Cam(10) Kan(50) Neo(50)
BMW349	Newman	pMW61; pTP63-SaDLT (dltD W130A)5	Cam(10)
BMW342	Newman	dltD::kan/ pMW61; pTP63-SaDLT (dltD W130A)5	Cam(10) Kan(50) Neo(50)
BMW354	Newman	pMW144; pTP63-SaDLT (myc-dltD S70C)1	Cam(10)
BMW364	Newman	dltD::kan/ pMW144; pTP63-SaDLT (myc-dltD S70C)1	Cam(10) Kan(50) Neo(50)
BMW359	Newman	pMW147; pTP63-SaDLT (myc-dltD D358C)1	Cam(10)

BMW360	Newman	dltD::kan/ pMW147; pTP63-SaDLT (myc-dltD D358C)1	Cam(10) Kan(50) Neo(50)
BMW355	Newman	pMW145; pTP63-SaDLT (myc-dltD Q129C)1	Cam(10)
BMW356	Newman	dltD::kan/ pMW145; pTP63-SaDLT (myc-dltD Q129C)1	Cam(10) Kan(50) Neo(50)
BMW357	Newman	pMW146; pTP63-SaDLT (myc-dltD W130C)1	Cam(10)
BMW358	Newman	dltD::kan/ pMW146; pTP63-SaDLT (myc-dltD W130C)1	Cam(10) Kan(50) Neo(50)
BMW406	Newman	pMW160; pTP63-SaDLT (myc-dltD E71A)1	Cam(10)
BMW407	Newman	dltD::kan/ pMW160; pTP63-SaDLT (myc-dltD E71A)1	Cam(10) Kan(50) Neo(50)
BMW408	Newman	pMW161; pTP63-SaDLT (myc-dltD E71Q)1	Cam(10)
BMW409	Newman	dltD::kan/ pMW161; pTP63-SaDLT (myc-dltD E71Q)1	Cam(10) Kan(50) Neo(50)
BMW428	Newman	pMW167; pTP63-SaDLT (myc-dltD E71N)	Cam(10)
BMW429	Newman	pMW167; dltD::kan/pTP63-SaDLT (myc-dltD E71N)	Cam(10) Kan(50) Neo(50)
BMW252	Newman	pMW98; pTP63-dltD1	Cam(10)
BMW253	Newman	dltD::kan/pMW98; pTP63-dltD1	Cam(10) Kan(50) Neo(50)
BMW176	Newman	pMW75; pTP63-SaDLT (dltB-myc)2	Cam(10)
BMW122	Newman	dltB::kanR/pTP63	Cam(10) Kan(50) Neo(50)
BMW197	Newman	dltB::kan/pMW75; pTP63-SaDLT (dltB-myc)2	Cam(10) Kan(50) Neo(50)
BMW320	Newman	pMW95; pTP63-SaDLT (dltB-myc H341A)1	Cam(10)
BMW321	Newman	dltB::kan/ pMW95; pTP63-SaDLT (dltB-myc H341A)1	Cam(10) Kan(50) Neo(50)
BMW240	Newman	pMW91; pTP63-SaDLT (dltB-myc H294A)1	Cam(10)
BMW249	Newman	dltB::kan/pMW91; pTP63-SaDLT (dltB-myc H294A)1	Cam(10) Kan(50) Neo(50)
BMW241	Newman	pMW93; pTP63-SaDLT (dltB-myc H294N)1	Cam(10)
BMW250	Newman	dltB::kan/pMW93; pTP63-SaDLT (dltB-myc H294N)1	Cam(10) Kan(50) Neo(50)
BMW400	Newman	pMW154; pTP63-myc-ltaS1	Cam(10)
BMW401	Newman	pMW156; pTP63-ltaS-myc1	Cam(10)
BMW391	Newman	dltD::kan/pMW154; pTP63-myc-ltaS1	Cam(10) Kan(50) Neo(50)
BMW392	Newman	dltD::kan/pMW156; pTP63-ltaS-myc1	Cam(10) Kan(50) Neo(50)
BMW422	Newman	pMW165; pTP63-myc-ltaS S218P2	Cam(10)
BMW423	Newman	pMW166; pTP63-ltaS-myc S218P1	Cam(10)
BMW424	Newman	dltD::kan/pMW165; pTP63-myc-ltaS S218P2	Cam(10) Kan(50) Neo(50)
BMW414	HG003	spa::tn-ErmR/ pMW154; pTP63-myc-ltaS1	Erm(5) Cam(10)
BMW415	HG003	spa::tn-ErmR/ pMW156; pTP63-ltaS-myc1	Erm(5) Cam(10)
BMW431	HG003	spa::tn-ErmR/ pMW166; pTP63-ltaS-myc S218P1	Erm(5) Cam(10)
BMW432	4S5	ΔltaS ΔgdpP dltD::kan	Kan(50) Neo(50)
		E. coli	
	XL1 Blue	tetR	Tet(10)
	BL21 (DE3)		
BMW27	BL21 (DE3)	pMW16; pET15b-dltA	Amp(100)
BMW28	BL21 (DE3)	pMW17; pET15b-dltB	Amp(100)
BMW29	BL21 (DE3)	pMW18; pET15b-dltD	Amp(100)
BMW30	BL21 (DE3)	pMW19; pET15b-dltDtrunc	Amp(100)
BMW33	BL21 (DE3)	pMW20; pET15b-dltC2	Amp(100)
BMW34	BL21 (DE3)	pMW21; pET15b-acpS	Amp(100)
BMW378	BL21 (DE3)	pMW149; pET15b-dltD Q129A	Amp(100)
BMW379	BL21 (DE3)	pMW150; pET15b-dltD Q129C	Amp(100)

BMW380	BL21 (DE3)	pMW151; pET15b-dltD W130A	Amp(100)
BMW381	BL21 (DE3)	pMW152; pET15b-dltD W130C	Amp(100)
BMW395	BL21 (DE3)	pMW138; pET15b-dltD S70A	Amp(100)
BMW396	BL21 (DE3)	pMW134; pET15b-dltD D358A	Amp(100)
BMW397	BL21 (DE3)	pMW139; pET15b-dltD H361A	Amp(100)
BMW412	BL21 (DE3)	pMW163; pET15b-dltD E71Q	Amp(100)
BMW413	BL21 (DE3)	pMW162; pET15b-dltD E71A	Amp(100)
BMW417	BL21 (DE3)	pMW164; pET15b-dltD E71N	Amp(100)

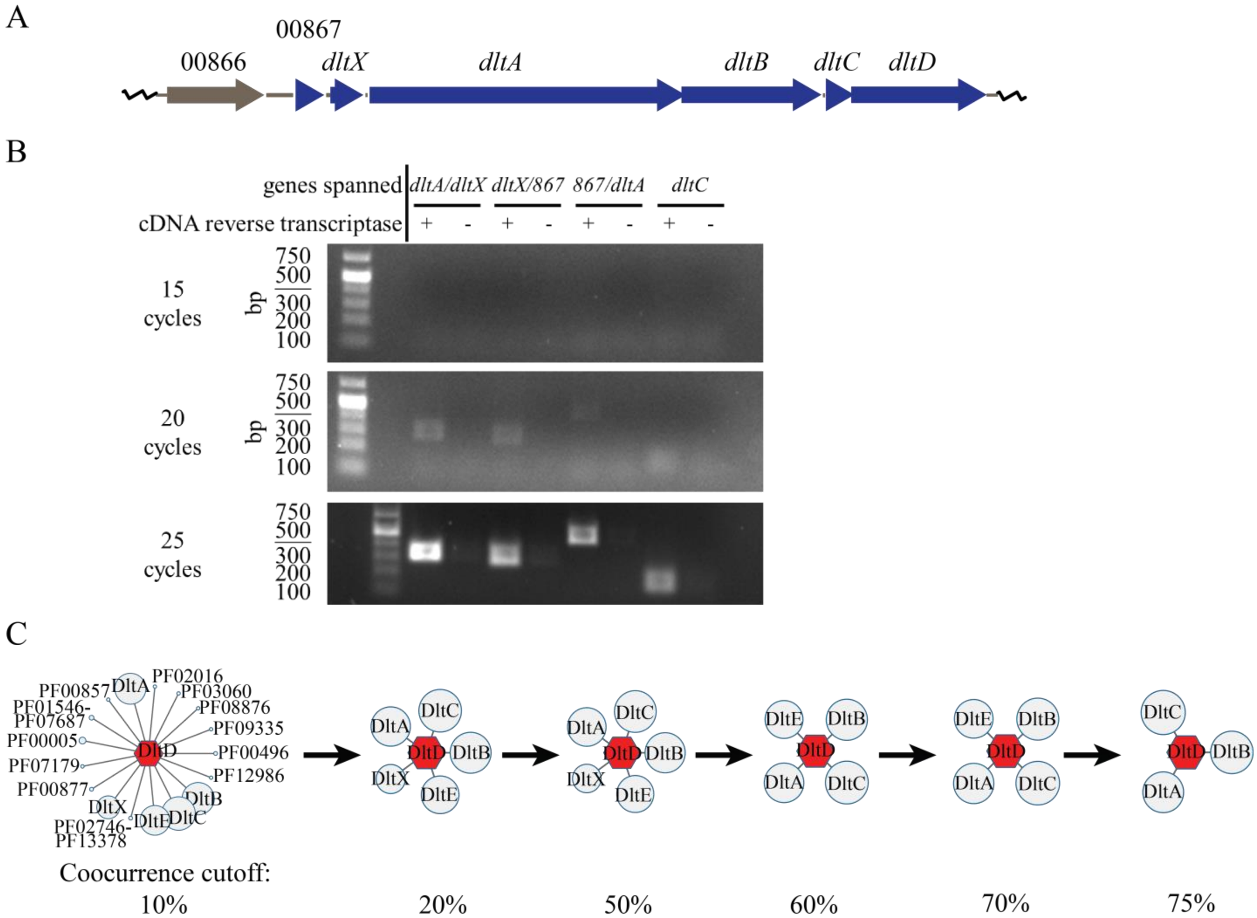

Figure S1. *The* S. aureus dlt *operon contains 6 genes while genome-neighborhood networks demonstrate a minimal, 4 gene operon.* Upstream of the recognized *dltABCD* operon is often found several genes in the same orientation. Neuhaus *et al.* stated that *dltE* and *dltX* "are not important for D-alanylation (Figure 9)"; however, no primary source was given (47). Previous studies showed that the farthest upstream gene, SAOUHSC_00866, is not co-transcribed with *dltABCD* (41). Panel A shows a cartoon of the putative operon structure in *S. aureus*. Here, we used rtPCR with primers spanning two genes each to test if the putative, upstream ORFs, SAOUHSC_00867 and SAOUHSC_00868 (dltX), are co-transcribed with *dltA*. Each sample of cDNA was prepared along with a separate "minus reverse transcriptase" sample to control for genomic DNA contamination. WT Newman cDNA (+ or - reverse transcriptase, RT) from cells grown to mid-log phase were tested with primers PMW240–PMW241 (dltX–dltA), PMW242–PMW243 (SAOUHSC_00867–dltX), PMW242–PMW241 (SAOUHSC_00867–dltA), and PMW154–PMW155 (dltC control). In Panel B, the results from 20 and 25 cycles clearly show a product for each pair of primers of the expected length without noticeable background in the -RT lanes. Also, test products formed at similar intensity cycle number as the *dltC* control reaction which would be expected if they were originating from the same mRNA. Therefore, the two ORFs upstream of *dltA* are part of the transcribed *dlt* operon. Lastly, a simple, statistical analysis was performed to test how often additional ORFs co-occur with *dltD*. The genome-neighborhood tool from the Enzyme Function Initiative (http://efi.igb.illinois.edu/efi-gnt/) was used with a Gram+ DltD SSN (PF04919) with a neighborhood size of 6 genes and varying cooccurrence cutoff stringencies to analyze the conservation of genes in the neighborhood of *dltD*. The red hexagonal node in the center of each network represents DltD, and the "spoke" nodes show proteins names or Pfam designations for genes cooccuring with DltD at a frequency less than or equal to the cutoff value indicated. Since *dltX* and *dltE* are present in less than 60% or 75% of dltD–encoding genomes, respectively, dltABCD are likely the only genes required for D-alanylation. The short ORF SAOUHSC_00867 is either not common enough to appear or is un-appreciated as an ORF in most encoding genomes.

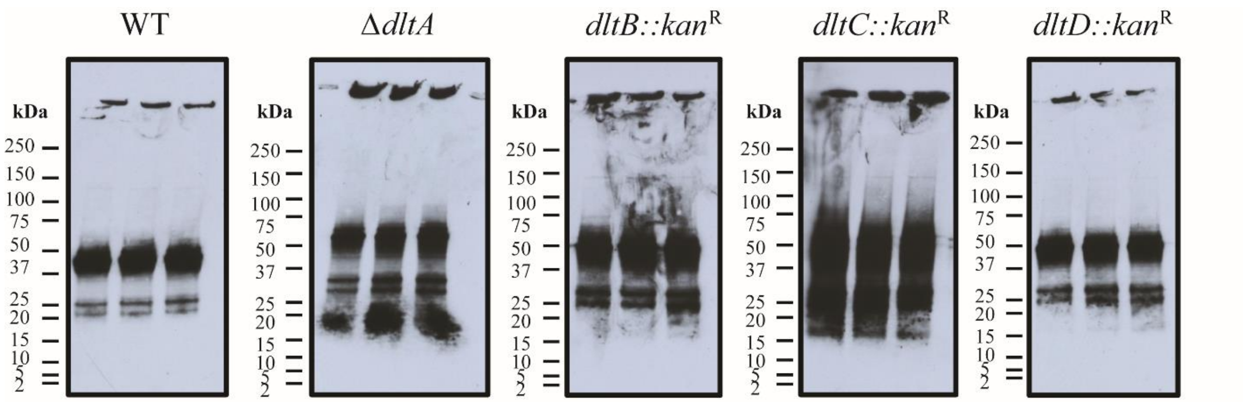

Figure S2. *Mutations in the dlt operon do not reduce LTA abundance*. Newman wildtype and *dlt* mutants were grown in TSB broth to OD ca. 1 before the cells were normalized to OD 1 and triplicate 0.1 mL aliquots were pelleted and frozen. Anti-polyglycerolphosphate (LTA) Western blot of the triplicate samples was carried-out similar to Grundling, *et. al* (48). The HRP-conjugate-containing blot was developed with ECL substrate and exposed to X-ray film. The 50 kDa band corresponds to protein A, and the 20 – 25 kDa smear is LTA.

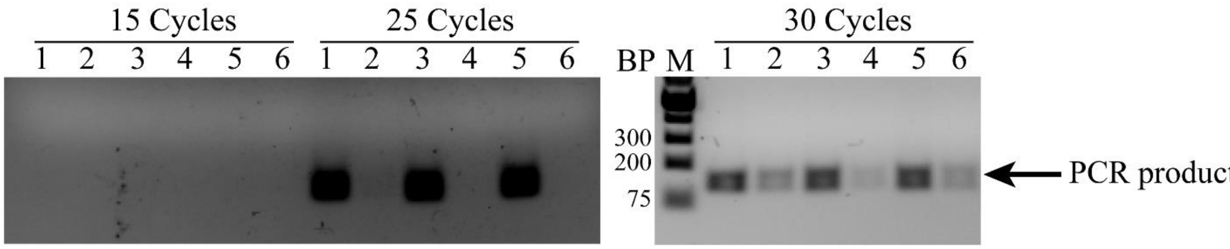

1. Newman wildtype with Reverse Transcriptase
2. Newman wildtype without Reverse Transcriptase
3. Newman Δ*dltB*::*kan* with RT
4. Newman Δ*dltB*::*kan* without RT
5. Newman Δ*dltD*::*kan* with RT
6. Newman Δ*dltD*::*kan* without RT

Figure S3. *Transcription of dltC is unaffected by the genetic deletion of dltB or dltD in those null mutants.* rtPCR was carried-out for the *dltC* gene from cDNA prepared from mid-log phase cultures of Newman WT, *dltB::kan*, and *dltD::kan* strains. Lanes 2, 4, and 6 contain samples to which reverse transcriptase was not added to the cDNA to show the level of DNA contamination in the RNA purifications. The PCR yield after 25 cycles from +RT cDNA samples for all three strains' mRNA look identical (no product at 15 cycles), so expression of *dltC* appears roughly unaffected in those two mutants. At 30 cycles, low levels of background product become apparent. All PCR reactions were identically prepared.

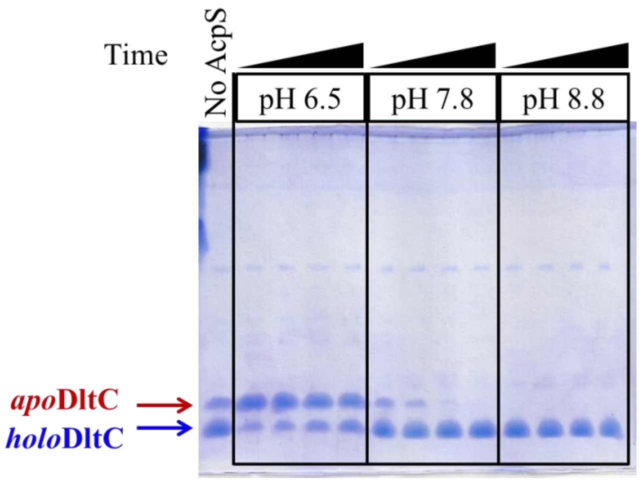

Figure S4. *Native PAGE analysis of* in vitro *phosphopantetheinylation of purified* S. aureus *DltC.* DltC purified from *E. coli* ran as two bands on 15% native PAGE following hexahistidine-tag cleavage by thrombin. A time course of AcpS-catalyzed phosphopantetheinylation was carried out at three different pH values, 6.5 (bisTris), 7.8 (Tris), and 8.8 (Tris), to observe conditions for preparation of *holo*DltC. After 0.5, 2, 5, 15 min, reactions containing 100 μM DltC, 250 μM CoA, and 3 μM AcpS were electrophoresed. Protein was imaged following Coomassie staining.

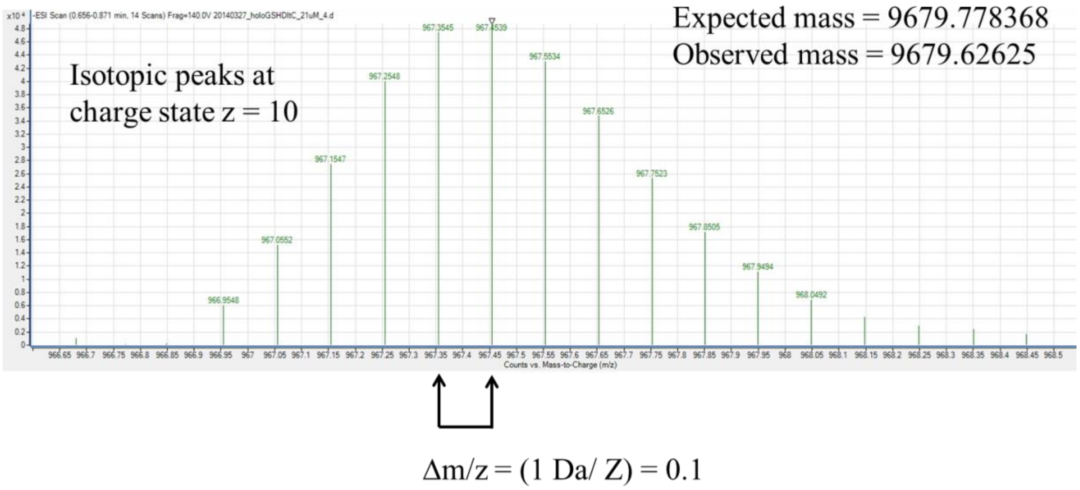

Figure S5. *MS analysis of holoDltC.* The thrombin cleaved and AcpS loaded holoDltC protein was analyzed by direct-infusion MS (Agilent 6520 Q-TOF) to confirm phosphopantetheinylation. The sequence of DltC (SAOUHSC_00871) was expected to be modified by the thrombin cleavage scar (*N*-terminal GlySerHis) which results from removal of the hexahistidine tag. Shown is a zoomed x-axis for isotope peaks corresponding to z = 10. The observed mass of 9679.62625 agrees well with the expected holo-GSH-DltC protein's expected mass, 9679.778368.

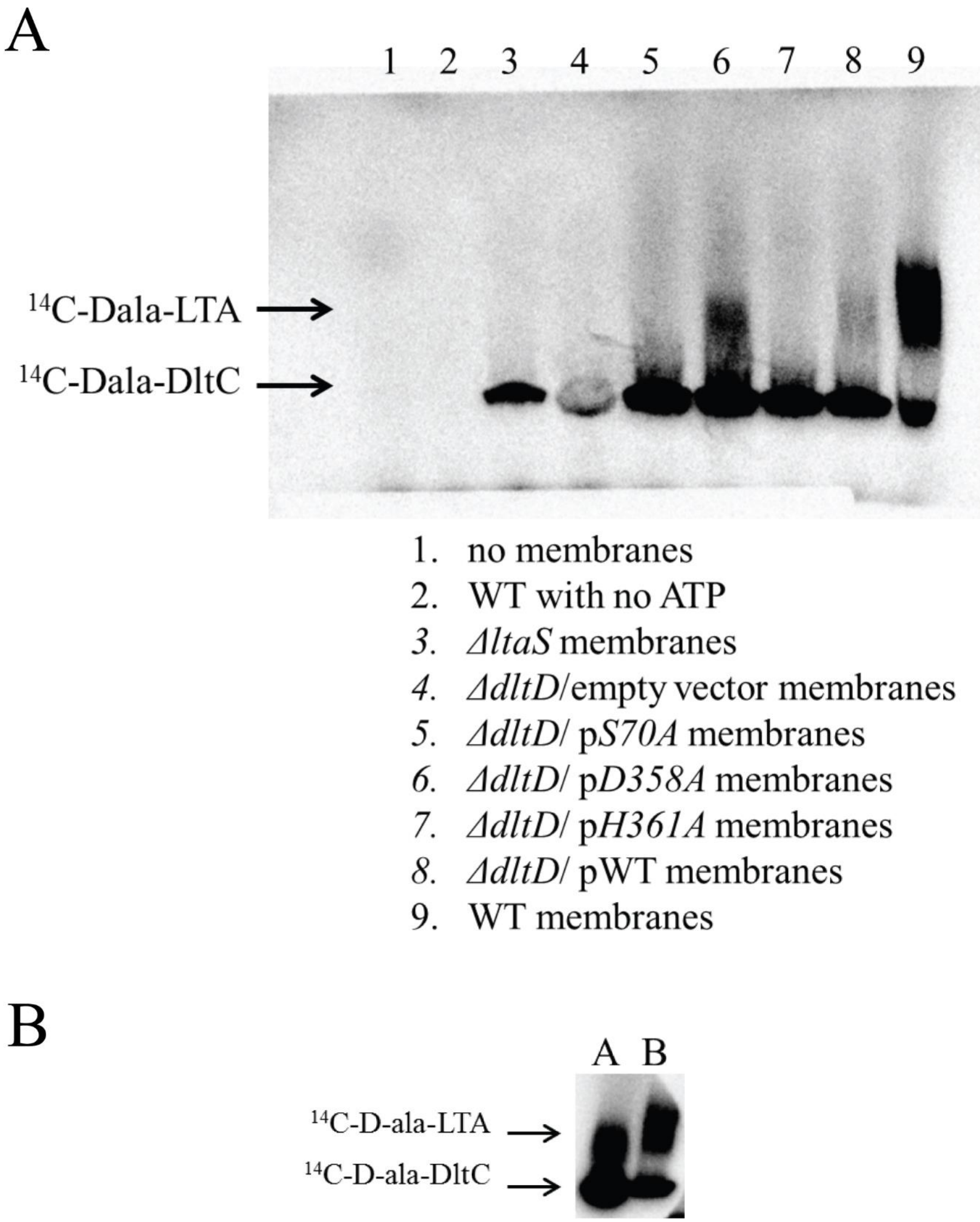

Figure S6. *Vesicles from complemented* dlt *null strains support* in vitro *LTA D-alanylation*. Vesicles prepared from fractionated membranes from a series of strains were incubated individually with ^{14}C-D-ala-DltC to test for LTA D-alanylation. In *Panel A*, Lanes 2 and 9 show vesicles from parent *S. aureus* Newman; while lanes 4 – 8 show the Newman *dltD* null strain with a series of plasmids. ^{14}C-D-ala-LTA formation can be seen for wild-type strain as well as DltD wild-type and D358A complemented *dltD* null strain. Lastly, no ^{14}C-D-ala-LTA formation was observed for vesicles prepared from the *ltaS* null strain, 4S5 (49). *Panel B* shows a separate test of whether purified DltD inserts into the membrane vesicles. Vesicles from dltD null mutant (Lane A) and wild-type Newman membranes (Lane B) (36 μg total membrane protein each) were mixed with 8 μM purified DltD and incubated at 30°C for 5 min before ultracentrifugation at 100,000 x g for 30 min. The reconstituted vesicles were then treated with ^{14}C-D-ala-DltC for 30 min before running on SDS-PAGE. The *dltD* null mutant with reconstituted DltD (Lane A) shows significant ^{14}C-D-ala-LTA formation compared to wild-type vesicles (Lane B). The slight difference in the apparent mobility of the two lanes is partially due to stretching of the gel during drying that resulted in the gel cracking.

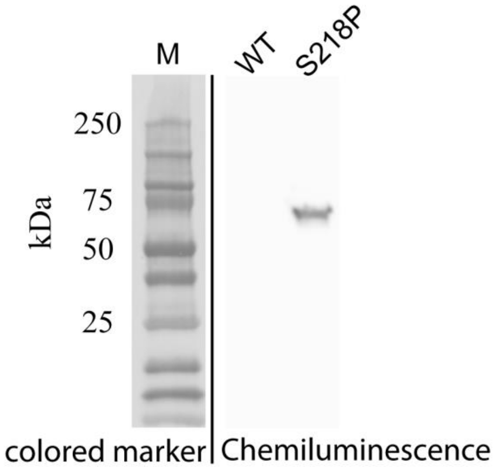

Figure S7 *LtaS is absent from vesicles due to site-specific cleavage*. LtaS was expressed from a plasmid in *S. aureus* with a C-terminal myc fusion. Wild-type LtaS was not detectible by Western blot in vesicles prepared from fractionated membranes of the same strain. The S218P mutant expressed with a C-terminal myc tag from the same plasmid and strain showed robust signal after vesicle preparation. Both vesicles were loaded at 37 µg of total membrane protein. Full length LtaS-myc is 76.8 kDa.

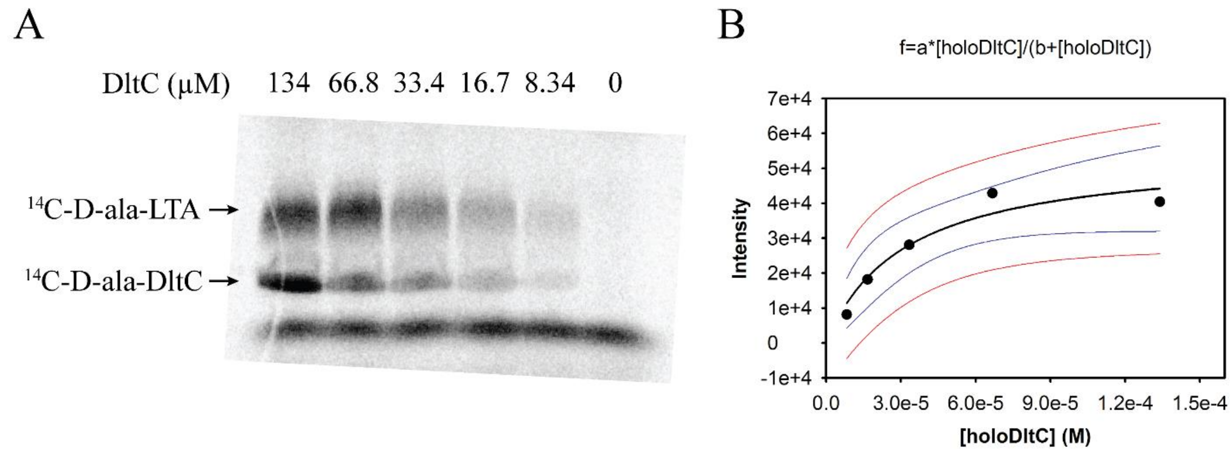

Figure S8. *Dependence of in vitro LTA D-alanylation on D-ala-holoDltC concentration.* The *in vitro* LTA D-alanylation assay was performed with varying concentrations from 0 to 134 μM DltC. Each DltA-catalyzed holoDltC charging reaction was preceded by DltA inactivation with MTSES (see *Experimental procedures*). Each ^{14}C-D-ala-*holo*DltC was then treated with the same amount of vesicles before 4 – 20% SDS-PAGE and autoradiography. Densitometry was performed using the software ImageJ, and the background corrected intensities for ^{14}C-D-ala-LTA were plotted against D-ala-*holo*DltC concentration. The data was fit to a rectangular hyperbola (blue line equals 95% confidence), and the following variables were calculated: a = 54632.6304 intensity units and b = 3.17E-05 M. The b value was taken as the concentration of ^{14}C-D-ala-*holo*DltC yielding 50% maximal *in vitro* LTA D-alanylation after 30 min.

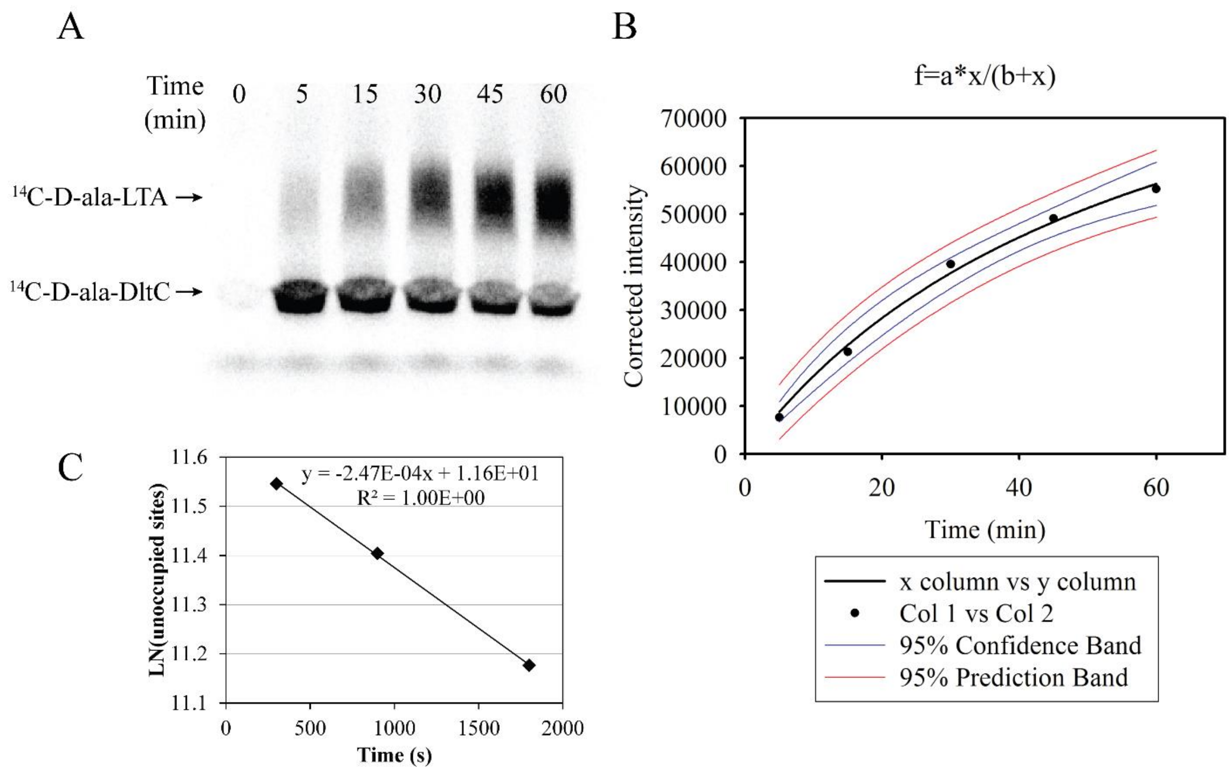

Figure S9. In vitro *LTA D-alanylation shows a half-life of approximately 50 min. In vitro* LTA D-alanylation with membrane-vesicles from wild type *S. aureus* was conducted over time course. DltA was quenched with 5 mM MTSES after DltC D-alanylation was complete but before initiation LTA D-alanylation by addition of membranes. Autoradiography from SDS-PAGE separated LTA was used for densitometry (representative exposure in *Panel A*). Normalized, background-corrected intensities from two different exposure times (to correct for limited dynamic range) was plotted against time to calculate the maximum possible intensity, a = 110981 (*Panel B*). This value was taken as the initial abundance of available LTA D-alanylation sites (A_O), and the difference between the intensity at each time point, t, and Ao yielded the remaining, unoccupied D-alanylation sites, A_t. The data between 5 and 30 min approached linearity, so the natural log of those values were used to calculate a first-order rate constant from a plot of $\ln(A_t) = -kt + \ln(A_O)$ (*Panel C*). A half-life for unoccupied LTA D-alanylation sites of 46.8 min was calculated from the rate constant, $k = 2.47 \times 10^{-4}\ s^{-1}$.

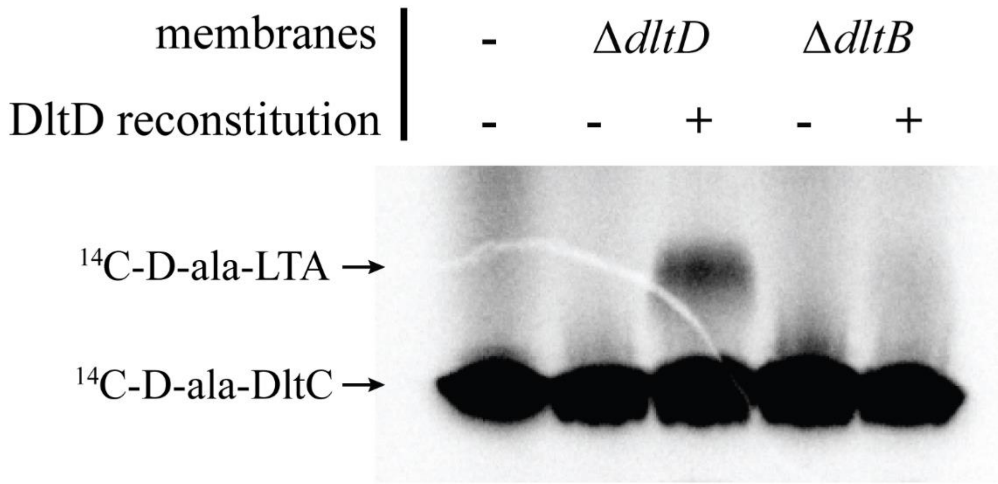

Figure S10. In vitro *LTA D-alanylation with DltD reconstituted membranes depends on the presence of DltB.* Purified, full length DltD was reincorporated into vesicles of membranes from a *dltD* null mutant (lanes 3) or a *dltB* null mutant (lanes 5) of *S. aureus*. DltC ^{14}C-D-alanylation by DltA *in vitro* without addition of DltD was carried-out in the presence (lanes 2 and 4) or absence (lane 1) of membranes. Thus, the ^{14}C-D-ala-LTA band was dependent on all DLT components, and DltC D-alanylation was independent of the membrane-bound steps. The dependence of LTA D-alanylation activity on the presence of DltB is evidence that the LTA D-alanylation *in vitro* is mechanistically the same as *in vivo* LTA D-alanylation, *i.e.*, DltD did not directly transfer D-alanine from DltC to LTA all on one face of the membrane.

A

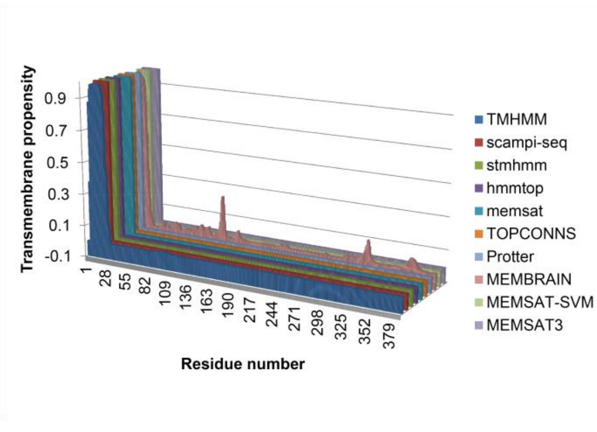

B.

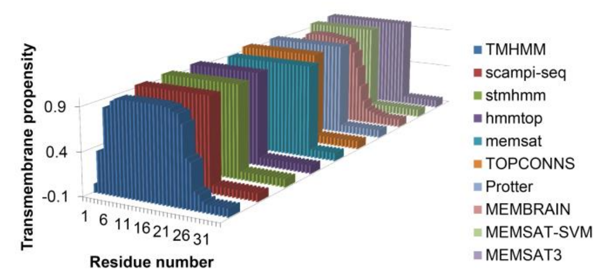

Figure S11. *DltD is predicted to contain one membrane spanning helix at the* N-*terminus.* The results from analysis of DltD's primary structure by several commonly used membrane protein topology prediction software were plotted above. The propensity to form a transmembrane helix at each residue was plotted across the entire polypeptide (*Panel A*), and the unanimous N-terminal helix is zoomed in *Panel B* (residues 7 and 27 based on an average of all results).

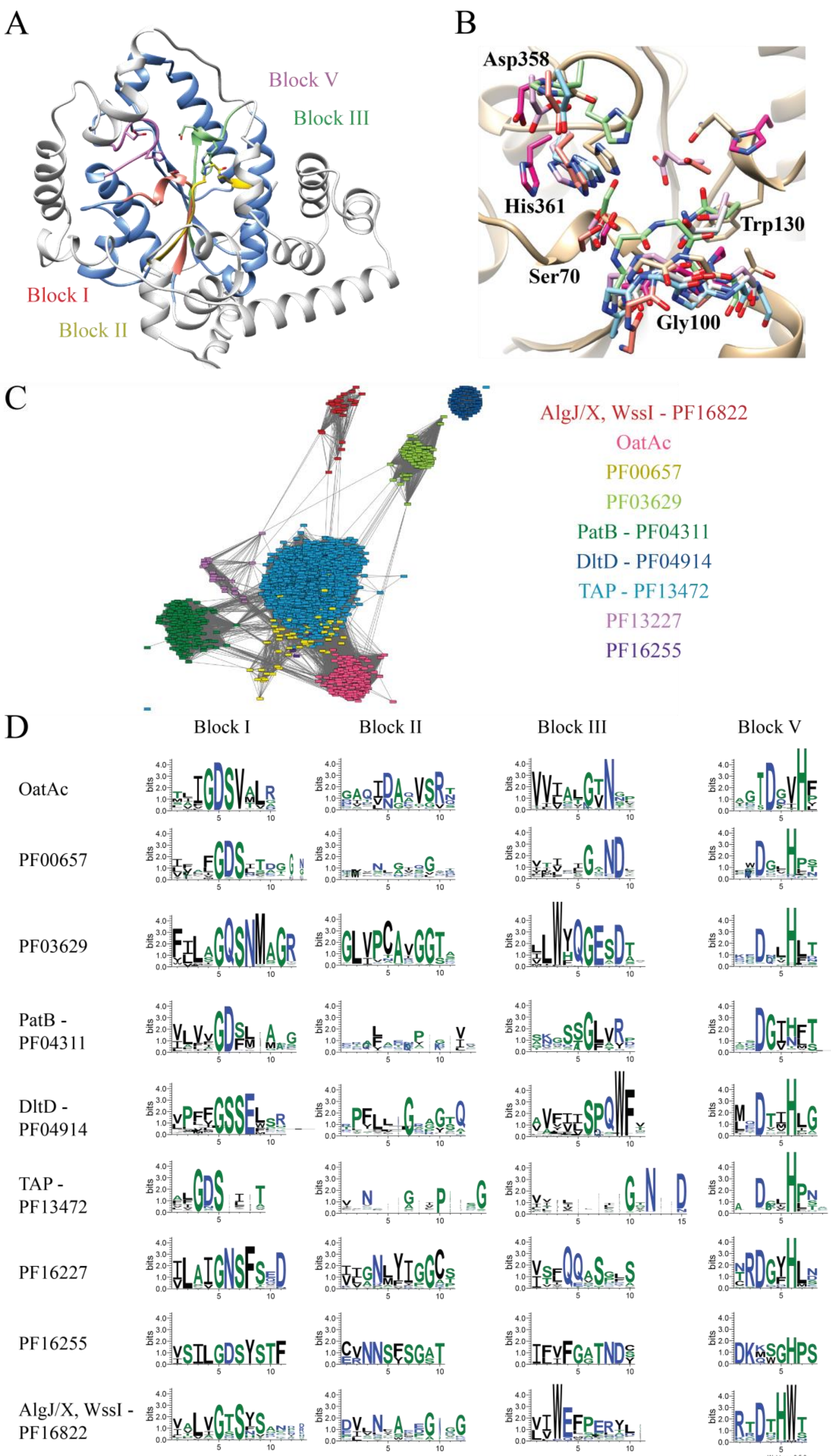
A
Block V
Block III
Block I
Block II
B
Asp358
His361
Trp130
Ser70
Gly100
C
AlgJ/X, WssI - PF16822
OatAc
PF00657
PF03629
PatB - PF04311
DltD - PF04914
TAP - PF13472
PF13227
PF16255
D
Block I
Block II
Block III
Block V
OatAc
PF00657
PF03629
PatB - PF04311
DltD - PF04914
TAP - PF13472
PF16227
PF16255
AlgJ/X, WssI - PF16822
WebLogo 3.5.0

Figure S12. *Conserved blocks of residues across SGNH-like proteins.* Analysis of proteins evolutionarily related to DltD was undertaken to gain insight into active site residues. In *Panel A*, the homology model of *S. aureus* DltD is colored to illustrate four blocks of residues which contribute to the active-site and which house the majority of the conserved residues. The greyed secondary structure includes the *N*-terminal transmembrane helix as well as the large insertion in the DltD protein, residues 133-282, relative to every other SGNH-family member. The blocks are colored salmon (Block I, residues 64 – 74), golden rod (Block II, residues 93 – 103), light green (Block III, residues 122 – 132), and orchid (Block V, residues 356 – 363) (all residue numbering corresponds to *S. aureus* DltD). For the top 40 hits from a DALI server query of DltD, each represented Pfam family was downloaded. Structural alignments of single representative structures for each family are shown in Panel B: DltD (tan, 3bma), TAP (blue, 1IVN, Z score = 10.3), EstA (pink, 1ZMB, Z score = 7.8), EstA-like (green, 3U37, Z score = 8.5), uncharacterized (salmon and grey, 4I8I (Z score = 8.0) and 4M8K (Z score = 9.4), and AlgX (pink, 4KNC). Structural alignments aided alignment of these divergent sequences and extraction of the conserved blocks of residues recognized for SGNH family proteins (50). Top BLAST hits for the *C*-terminal domain of OatA, which was independently identified as an SGNH-like protein, were separately downloaded and aligned because structures and Pfam designations were both lacking for this domain. Because of the low sequence identity (and insertions, *e.g.*, DltD, or structural rearrangement, *i.e.*, AlgJ/AlgX/WssI proteins) between all of these proteins, each of the four extracted blocks of residues for each protein were joined into polypeptide sequences of 30-40 amino acids (5134 total sequences), and they were A) submitted as a custom database to the EFI-EST server (http://efi.igb.illinois.edu/efi-est/) and B) aligned *via* MUSCLE for manual analysis. The resulting sequence similarity network is shown in *Panel C*. The sequence divergence of DltD is sufficiently far from the rest of the SGNH-like proteins that DltD sequences do not connect with the other families in the network at the lenient all-by-all BLAST E value cutoff of 0.1. The other known or proposed transferases, *i.e.*, AlgJ/X/WssI, PatB, OatAc, all show connections to the large hydrolase family, PF13472, which includes the *E. coli* TAP. This suggests that a transferase evolved from a hydrolase one or more times in this large, putative family and provides proof-of-principle for DltD's proposed evolutionary origins. In *Panel D*, the MUSCLE alignments are illustrated as sequence logo representations of each block for each family. The meaning of colors is not consistent across panels, and the colors in *Panel D* do not represent any chemical property. This analysis shows the catalytic triad (S7 Block I and D3 and H6 of Block V – extracted DltD numbering) as well as the turn before the S7 (G5 of Block I) to be extremely important across these diverse enzymes. The Asp of the catalytic triad appears to be less well conserved than His because the Block V DxxH motif also appears as a DxH motif (e.g., the AlgX-like proteins, Pfam family PF16822) or the Asp is missing all together (scattered examples). The oxyanion hole contributor at G7 of Block II is also shown to be important. Lastly, the titular Asn, *e.g.*, N12 of Block III for PF13472, for which the SG'N'H family is named, is lacking in many families including DltD, so the SGNH term is a misnomer. Taken together, it is possible that the DltD family is part of this family albeit the most divergent subfamily.

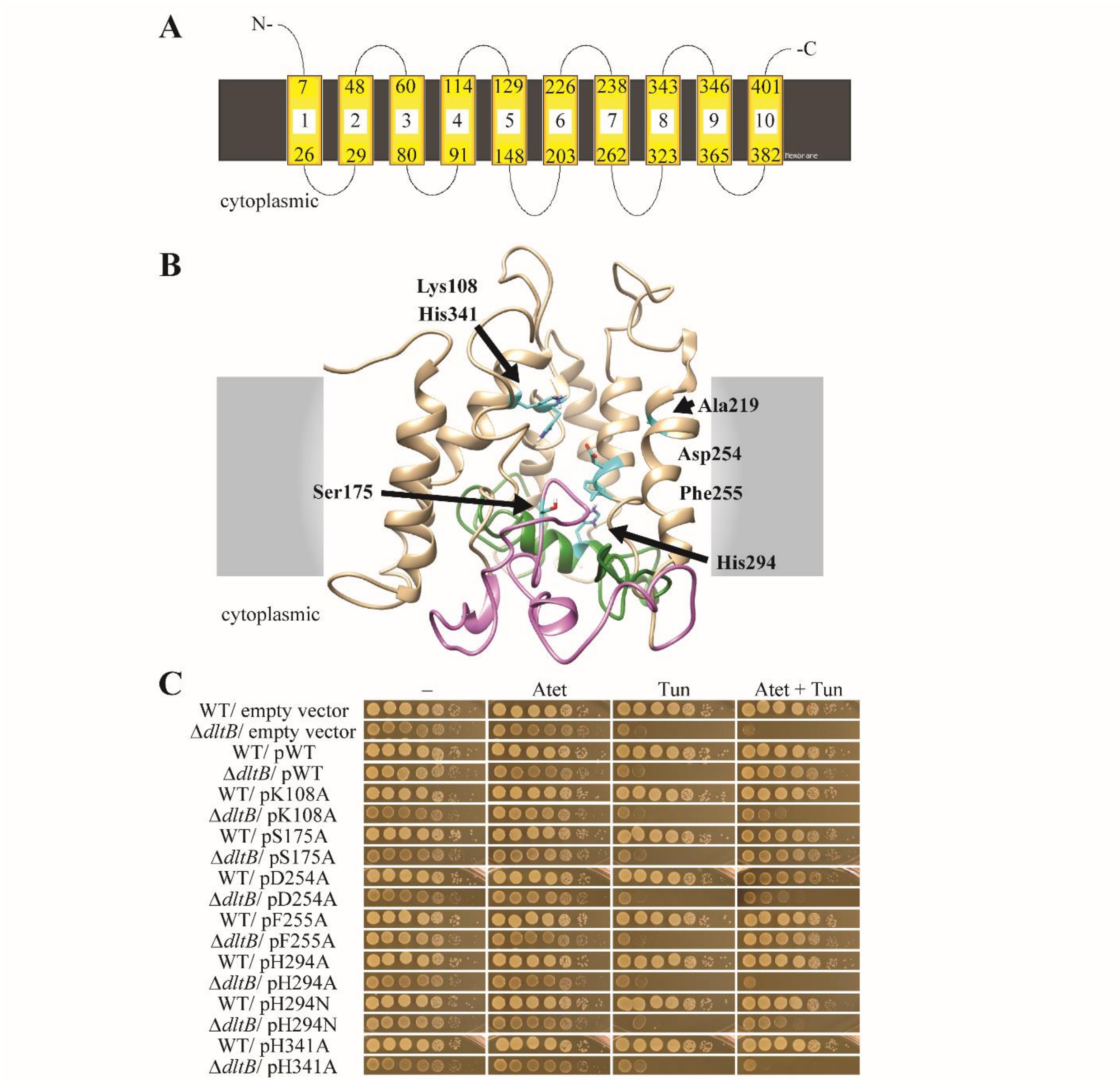

Figure S13. *Tunicamycin-DLT synthetic lethality assay uncovers residues important to DltB function.* As was performed for DltD, the topology of DltB was predicted with several programs. *Panel A* shows the result from MEMSAT3. In short, among the programs shown for DltD topology prediction, MEMSAT3 yielded the most consistent results among bacterial MBOAT family members in the conserved region from TM helices 4 – 9, and the prediction roughly agrees with a MUSCLE alignment to the well-studied MBOAT, GOAT. GOAT was found to have a reentrant loop that aligns with DltB's 100–153 cytoplasmic loop. From structural prediction using covariance analysis, this region was found to lie partially in the membrane for DltB as well (purple ribbons in *Panel B*, <evfold.org/evfold-web/newprediction.do>). Covariance analysis measures evolutionary pressure on pairs of residues across a family of related proteins based on their propensity to co-occur in particular pairs (51). Covariance can result from evolutionarily conserved, physical interactions within a protein. Also shown in *Panel B* in dark green is a second apparent reentrant loop at the cytoplasmic face of the membrane from residues 214-273. This loop is densely populated with conserved residues in DltB orthologs including the His294 which is conserved as a His or Asn throughout the MBOAT family. These two loops appear to form interactions with residues on transmembrane helices which may allow formation of a pocket for D-ala-DltC to bind. Besides the conserved MBOAT residues, His294 and His341, Panel B also shows the position of residues found mutated in Amsacrine resistant strains selected in the lab: Ser175, Ala219, and Phe255 (29). Site-directed mutagenesis of these residues as well as additional residues guided by the structural model was performed. In *Panel C*, WT and mutant *dltB* expressed off of an integrative vector as part of the *dltABCD* operon were tested for complementation of *dltB* null strain growth in the presence of 1 µg/mL tunicamycin. Tunicamycin (Tun) was added for synthetic lethal DLT selection, and Anhydrotetracycline (Atet) was added to 0.4 µM for induction off the integrative vector. H294A and H341A were completely inactive as found for other MBOAT family members. Most MBOAT proteins contain an asparagine at the His294 position, and the H294N mutation regained activity relative to the alanine mutant. The alanine-substitution at the amsacrine associated residues, Ser175 and Phe255, displayed WT activity. The nearby Asp254 showed reduced activity when mutated to alanine possibly suggesting the placement of Asp254 and Phe255 in the model near the center of the protein to be correct. Another residue predicted to be juxtaposed next to His341, Lys108, was found to also lower activity in DltB upon substitution to alanine.

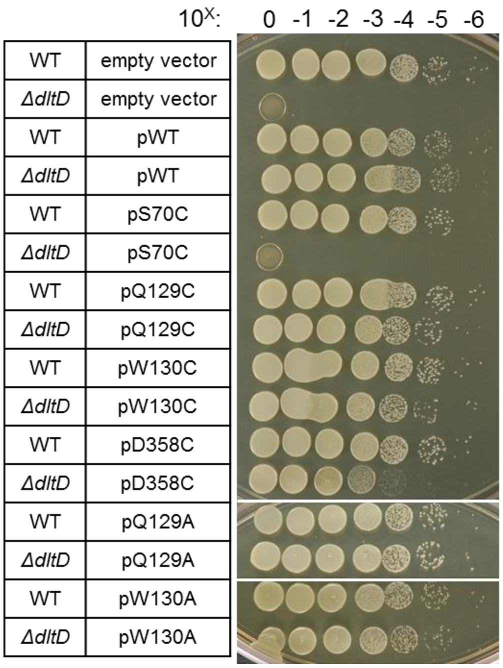

Figure S14. *Cysteine substitution of residues Q129 and W130 were active by tunicamycin growth complementation.* The cell-based assay for DLT activity by complementation of growth of *dlt* null mutants in the presence of tunicamycin (see Materials and Methods) was used to assess the activity in site-directed mutants of DltD in which Q129 and W130 were substituted to alanine or cysteine. None of the four mutants showed a loss of activity relative to wild-type. Additional cysteine mutants at the putative catalytic residues Ser70 and Asp358 showed a significant effect on growth, with a complete loss of activity seen for S70C.

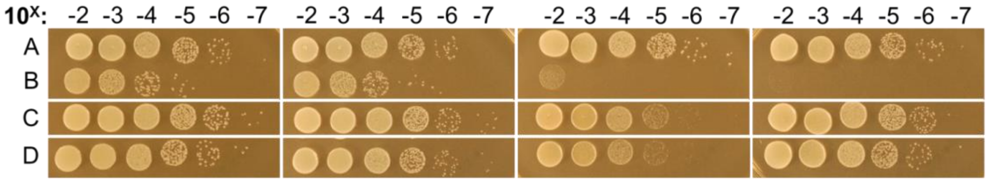

Figure S15. *DltD activity is unaffected by an N-terminal myc-tag.* *S. aureus* wild-type (A) and a dltD null mutant (B, C, and D) were transformed with either empty vector (A – B) or a plasmid containing the whole *dlt* operon with native *dltD* (C) or *dltD* fused with an *N*-terminal myc-tag (D). The native and myc-tagged constructs provide equal growth complementation in the presence of tunicamycin (Tun). Wall teichoic acid biosynthesis and the *dlt* operon are synthetically lethal, so treatment with the TarO inhibitor, tunicamycin, creates a *dlt*-selective condition. Anhydrotetracycline (Atet) induced the expression of the *dlt* operon from a plasmid, so comparison of Tun sensitivity with and without expression shows the specificity of the growth complementation to the *dlt* expression.

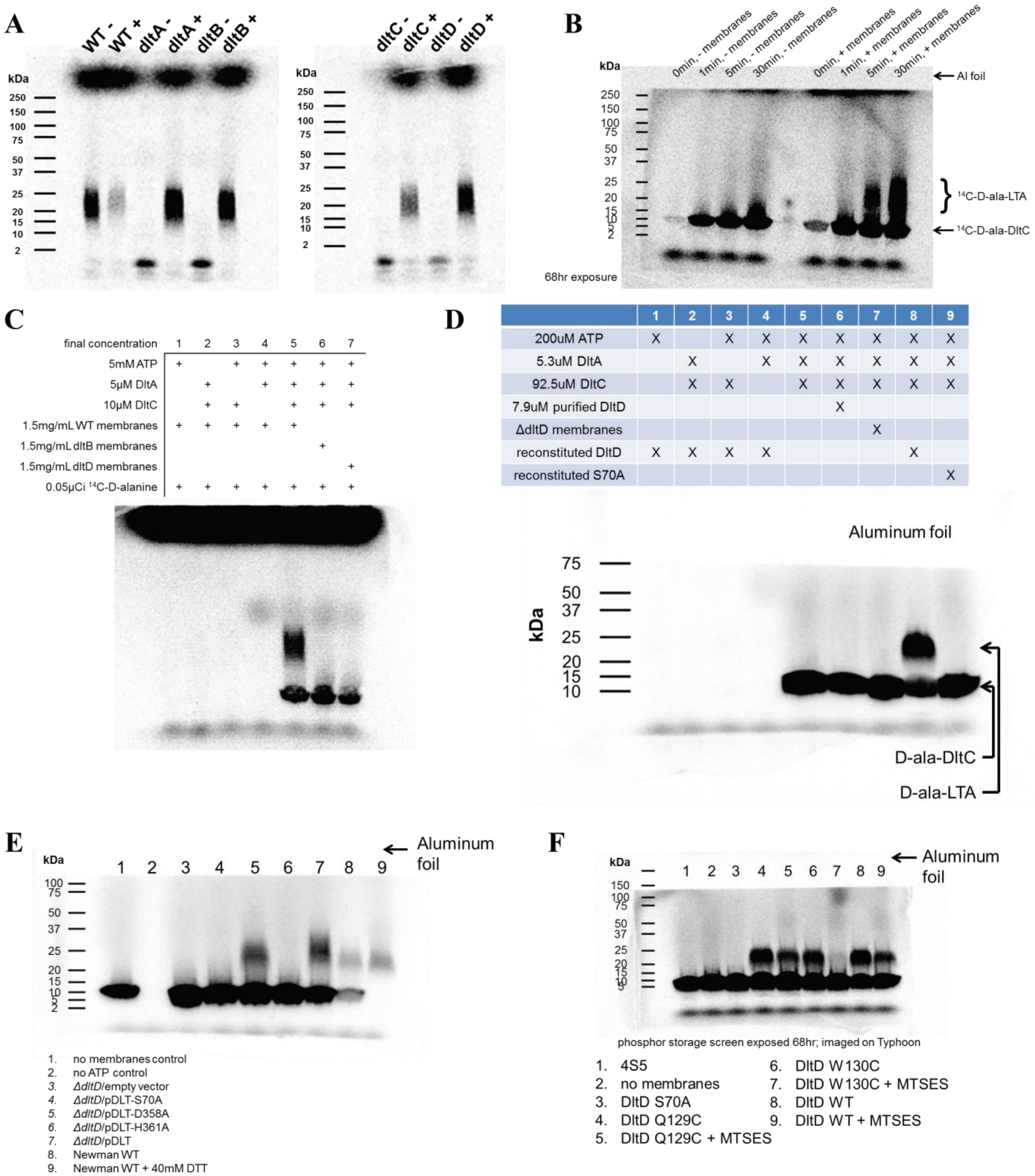

Figure S16. *Full gels from main text figures*. Figure 2 *Panel C* is shown in in *Panel A*. The inset of Figure 3 *Panel A* and *Panels B* and *C* are shown here in *Panel B*, *C*, and *D*, respectively. Lastly, Figure 5 *Panels C and D* are shown here in *Panels E* and *F*, respectively.

References

1. Perego, M., Glaser, P., Minutello, A., Strauch, M. A., Leopold, K., and Fischer, W. (1995) Incorporation of D-Alanine into Lipoteichoic Acid and Wall Teichoic Acid in Bacillus subtilis IDENTIFICATION OF GENES AND REGULATION. *J. Biol. Chem.* **270**, 15598–15606
2. Peschel, A., Otto, M., Jack, R. W., Kalbacher, H., Jung, G., and Götz, F. (1999) Inactivation of the dlt Operon inStaphylococcus aureus Confers Sensitivity to Defensins, Protegrins, and Other Antimicrobial Peptides. *J. Biol. Chem.* **274**, 8405–8410
3. Clemans, D. L., Kolenbrander, P. E., Debabov, D. V., Zhang, Q., Lunsford, R. D., Sakone, H., Whittaker, C. J., Heaton, M. P., and Neuhaus, F. C. (1999) Insertional Inactivation of Genes Responsible for the d-Alanylation of Lipoteichoic Acid in Streptococcus gordonii DL1 (Challis) Affects Intrageneric Coaggregations. *Infect. Immun.* **67**, 2464–2474
4. Boyd, D. A., Cvitkovitch, D. G., Bleiweis, A. S., Kiriukhin, M. Y., Debabov, D. V., Neuhaus, F. C., and Hamilton, I. R. (2000) Defects in d-Alanyl-Lipoteichoic Acid Synthesis in Streptococcus mutans Results in Acid Sensitivity. *J. Bacteriol.* **182**, 6055–6065
5. Nilsson, M., Rybtke, M., Givskov, M., Høiby, N., Twetman, S., and Tolker-Nielsen, T. (2016) The dlt genes play a role in antimicrobial tolerance of Streptococcus mutans biofilms. *Int. J. Antimicrob. Agents*. **48**, 298–304
6. Kovács, M., Halfmann, A., Fedtke, I., Heintz, M., Peschel, A., Vollmer, W., Hakenbeck, R., and Brückner, R. (2006) A functional dlt operon, encoding proteins required for incorporation of d-alanine in teichoic acids in gram-positive bacteria, confers resistance to cationic antimicrobial peptides in Streptococcus pneumoniae. *J. Bacteriol.* **188**, 5797–5805
7. Kristian, S. A., Datta, V., Weidenmaier, C., Kansal, R., Fedtke, I., Peschel, A., Gallo, R. L., and Nizet, V. (2005) d-Alanylation of Teichoic Acids Promotes Group A Streptococcus Antimicrobial Peptide Resistance, Neutrophil Survival, and Epithelial Cell Invasion. *J. Bacteriol.* **187**, 6719–6725
8. Debabov, D. V., Kiriukhin, M. Y., and Neuhaus, F. C. (2000) Biosynthesis of Lipoteichoic Acid in Lactobacillus rhamnosus: Role of DltD in d-Alanylation. *J. Bacteriol.* **182**, 2855–2864
9. McBride, S. M., and Sonenshein, A. L. (2011) The dlt operon confers resistance to cationic antimicrobial peptides in Clostridium difficile. *Microbiology*. **157**, 1457–1465
10. Fabretti, F., Theilacker, C., Baldassarri, L., Kaczynski, Z., Kropec, A., Holst, O., and Huebner, J. (2006) Alanine Esters of Enterococcal Lipoteichoic Acid Play a Role in Biofilm Formation and Resistance to Antimicrobial Peptides. *Infect. Immun.* **74**, 4164–4171
11. Peschel, A., Vuong, C., Otto, M., and Götz, F. (2000) The D-alanine residues of Staphylococcus aureus teichoic acids alter the susceptibility to vancomycin and the activity of autolytic enzymes. *Antimicrob. Agents Chemother.* **44**, 2845–2847
12. Matsuo, M., Oogai, Y., Kato, F., Sugai, M., and Komatsuzawa, H. (2011) Growth-phase dependence of susceptibility to antimicrobial peptides in Staphylococcus aureus. *Microbiology*. **157**, 1786–1797
13. Simanski, M., Gläser, R., Köten, B., Meyer-Hoffert, U., Wanner, S., Weidenmaier, C., Peschel, A., and Harder, J. (2013) Staphylococcus aureus subverts cutaneous defense by D-alanylation of teichoic acids. *Exp. Dermatol.* **22**, 294–296
14. Blake, K. L., and O'Neill, A. J. (2013) Transposon library screening for identification of genetic loci participating in intrinsic susceptibility and acquired resistance to antistaphylococcal agents. *J. Antimicrob. Chemother.* **68**, 12–16
15. Mazda, Y., Kawada-Matsuo, M., Kanbara, K., Oogai, Y., Shibata, Y., Yamashita, Y., Miyawaki, S., and Komatsuzawa, H. (2012) Association of CiaRH with resistance of Streptococcus mutans to antimicrobial peptides in biofilms. *Mol. Oral Microbiol.* **27**, 124–135
16. Poyart, C., Pellegrini, E., Marceau, M., Baptista, M., Jaubert, F., Lamy, M.-C., and Trieu-Cuot, P. (2003) Attenuated virulence of Streptococcus agalactiae deficient in D-alanyl-lipoteichoic acid is due to an increased susceptibility to defensins and phagocytic cells. *Mol. Microbiol.* **49**, 1615–1625

17. Saar-Dover, R., Bitler, A., Nezer, R., Shmuel-Galia, L., Firon, A., Shimoni, E., Trieu-Cuot, P., and Shai, Y. (2012) D-Alanylation of Lipoteichoic Acids Confers Resistance to Cationic Peptides in Group B Streptococcus by Increasing the Cell Wall Density. *PLOS Pathog.* **8**, e1002891
18. Perea Vélez, M., Verhoeven, T. L. A., Draing, C., Von Aulock, S., Pfitzenmaier, M., Geyer, A., Lambrichts, I., Grangette, C., Pot, B., Vanderleyden, J., and De Keersmaecker, S. C. J. (2007) Functional analysis of D-alanylation of lipoteichoic acid in the probiotic strain Lactobacillus rhamnosus GG. *Appl. Environ. Microbiol.* **73**, 3595–3604
19. Walter, J., Loach, D. M., Alqumber, M., Rockel, C., Hermann, C., Pfitzenmaier, M., and Tannock, G. W. (2007) D-alanyl ester depletion of teichoic acids in Lactobacillus reuteri 100-23 results in impaired colonization of the mouse gastrointestinal tract. *Environ. Microbiol.* **9**, 1750–1760
20. Revilla-Guarinos, A., Gebhard, S., Alcántara, C., Staron, A., Mascher, T., and Zúñiga, M. (2013) Characterization of a regulatory network of peptide antibiotic detoxification modules in Lactobacillus casei BL23. *Appl. Environ. Microbiol.* **79**, 3160–3170
21. Abachin, E., Poyart, C., Pellegrini, E., Milohanic, E., Fiedler, F., Berche, P., and Trieu-Cuot, P. (2002) Formation of D-alanyl-lipoteichoic acid is required for adhesion and virulence of Listeria monocytogenes. *Mol. Microbiol.* **43**, 1–14
22. Cafiso, V., Bertuccio, T., Purrello, S., Campanile, F., Mammina, C., Sartor, A., Raglio, A., and Stefani, S. (2014) dltA overexpression: A strain-independent keystone of daptomycin resistance in methicillin-resistant Staphylococcus aureus. *Int. J. Antimicrob. Agents*. **43**, 26–31
23. Mishra, N. N., Bayer, A. S., Weidenmaier, C., Grau, T., Wanner, S., Stefani, S., Cafiso, V., Bertuccio, T., Yeaman, M. R., Nast, C. C., and Yang, S.-J. (2014) Phenotypic and Genotypic Characterization of Daptomycin-Resistant Methicillin-Resistant Staphylococcus aureus Strains: Relative Roles of mprF and dlt Operons. *PLOS ONE*. **9**, e107426
24. Mechler, L., Bonetti, E.-J., Reichert, S., Flötenmeyer, M., Schrenzel, J., Bertram, R., François, P., and Götz, F. (2016) Daptomycin Tolerance in the Staphylococcus aureus pitA6 Mutant Is Due to Upregulation of the dlt Operon. *Antimicrob. Agents Chemother.* **60**, 2684–2691
25. Kang, K.-M., Mishra, N. N., Park, K. T., Lee, G.-Y., Park, Y. H., Bayer, A. S., and Yang, S.-J. (2017) Phenotypic and genotypic correlates of daptomycin-resistant methicillin-susceptible Staphylococcus aureus clinical isolates. *J. Microbiol. Seoul Korea*. **55**, 153–159
26. Wecke, J., Madela, K., and Fischer, W. (1997) The absence of D-alanine from lipoteichoic acid and wall teichoic acid alters surface charge, enhances autolysis and increases susceptibility to methicillin in Bacillus subtilis. *Microbiology*. **143**, 2953–2960
27. Nakao, A., Imai, S., and Takano, T. (2000) Transposon-mediated insertional mutagenesis of the D-alanyl-lipoteichoic acid (dlt) operon raises methicillin resistance in Staphylococcus aureus. *Res. Microbiol.* **151**, 823–829
28. Maria, J. P. S., Sadaka, A., Moussa, S. H., Brown, S., Zhang, Y. J., Rubin, E. J., Gilmore, M. S., and Walker, S. (2014) Compound-gene interaction mapping reveals distinct roles for Staphylococcus aureus teichoic acids. *Proc. Natl. Acad. Sci.* **111**, 12510–12515
29. Pasquina, L., Santa Maria Jr, J. P., McKay Wood, B., Moussa, S. H., Matano, L. M., Santiago, M., Martin, S. E. S., Lee, W., Meredith, T. C., and Walker, S. (2016) A synthetic lethal approach for compound and target identification in Staphylococcus aureus. *Nat. Chem. Biol.* **12**, 40–45
30. Bensaci, M. F., and Takemoto, J. Y. (2007) Syringopeptin SP25A-mediated killing of gram-positive bacteria and the role of teichoic acid d-alanylation. *FEMS Microbiol. Lett.* **268**, 106–111
31. Koprivnjak, T., Peschel, A., Gelb, M. H., Liang, N. S., and Weiss, J. P. (2002) Role of Charge Properties of Bacterial Envelope in Bactericidal Action of Human Group IIA Phospholipase A2against Staphylococcus aureus. *J. Biol. Chem.* **277**, 47636–47644

32. Guariglia-Oropeza, V., and Helmann, J. D. (2011) Bacillus subtilis σV Confers Lysozyme Resistance by Activation of Two Cell Wall Modification Pathways, Peptidoglycan O-Acetylation and d-Alanylation of Teichoic Acids ▿. *J. Bacteriol.* **193**, 6223–6232
33. Herbert, S., Bera, A., Nerz, C., Kraus, D., Peschel, A., Goerke, C., Meehl, M., Cheung, A., and Götz, F. (2007) Molecular Basis of Resistance to Muramidase and Cationic Antimicrobial Peptide Activity of Lysozyme in Staphylococci. *PLOS Pathog.* **3**, e102
34. Wecke, J., Perego, M., and Fischer, W. (1996) D-alanine deprivation of Bacillus subtilis teichoic acids is without effect on cell growth and morphology but affects the autolytic activity. *Microb. Drug Resist. Larchmt. N*. **2**, 123–129
35. Steen, A., Palumbo, E., Deghorain, M., Cocconcelli, P. S., Delcour, J., Kuipers, O. P., Kok, J., Buist, G., and Hols, P. (2005) Autolysis of Lactococcus lactis Is Increased upon d-Alanine Depletion of Peptidoglycan and Lipoteichoic Acids. *J. Bacteriol.* **187**, 114–124
36. Archibald, A. R., Baddiley, J., and Heptinstall, S. (1973) The alanine ester content and magnesium binding capacity of walls of Staphylococcus aureus H grown at different pH values. *Biochim. Biophys. Acta*. **291**, 629–634
37. MacArthur, A. E., and Archibald, A. R. (1984) Effect of culture pH on the D-alanine ester content of lipoteichoic acid in Staphylococcus aureus. *J. Bacteriol.* **160**, 792–793
38. Revilla-Guarinos, A., Alcántara, C., Rozès, N., Voigt, B., and Zúñiga, M. (2014) Characterization of the response to low pH of Lactobacillus casei ΔRR12, a mutant strain with low D-alanylation activity and sensitivity to low pH. *J. Appl. Microbiol.* **116**, 1250–1261
39. Gross, M., Cramton, S. E., Götz, F., and Peschel, A. (2001) Key Role of Teichoic Acid Net Charge in Staphylococcus aureus Colonization of Artificial Surfaces. *Infect. Immun.* **69**, 3423–3426
40. Hyyryläinen, H.-L., Vitikainen, M., Thwaite, J., Wu, H., Sarvas, M., Harwood, C. R., Kontinen, V. P., and Stephenson, K. (2000) d-Alanine Substitution of Teichoic Acids as a Modulator of Protein Folding and Stability at the Cytoplasmic Membrane/Cell Wall Interface of Bacillus subtilis. *J. Biol. Chem.* **275**, 26696–26703
41. Koprivnjak, T., Mlakar, V., Swanson, L., Fournier, B., Peschel, A., and Weiss, J. P. (2006) Cation-Induced Transcriptional Regulation of the dlt Operon of Staphylococcus aureus. *J. Bacteriol.* **188**, 3622–3630
42. Kaito, C., and Sekimizu, K. (2007) Colony Spreading in Staphylococcus aureus. *J. Bacteriol.* **189**, 2553–2557
43. Fischer, W., and Rösel, P. (1980) The alanine ester substitution of lipoteichoic acid (LTA) in Staphylococcus aureus. *FEBS Lett.* **119**, 224–226
44. Collins, L. V., Kristian, S. A., Weidenmaier, C., Faigle, M., Kessel, V., M, K. P., Strijp, V., G, J. A., Götz, F., Neumeister, B., and Peschel, A. (2002) Staphylococcus aureus Strains Lacking d-Alanine Modifications of Teichoic Acids Are Highly Susceptible to Human Neutrophil Killing and Are Virulence Attenuated in Mice. *J. Infect. Dis.* **186**, 214–219
45. Wobser, D., Ali, L., Grohmann, E., Huebner, J., and Sakinc, T. (2014) A Novel Role for D-Alanylation of Lipoteichoic Acid of Enterococcus faecalis in Urinary Tract Infection. *PLOS ONE*. **9**, e107827
46. Weidenmaier, C., McLoughlin, R. M., and Lee, J. C. (2010) The Zwitterionic Cell Wall Teichoic Acid of Staphylococcus aureus Provokes Skin Abscesses in Mice by a Novel CD4+ T-Cell-Dependent Mechanism. *PLoS ONE*. 10.1371/journal.pone.0013227
47. Neuhaus, F. C., and Baddiley, J. (2003) A Continuum of Anionic Charge: Structures and Functions of d-Alanyl-Teichoic Acids in Gram-Positive Bacteria. *Microbiol. Mol. Biol. Rev.* **67**, 686–723
48. Gründling, A., and Schneewind, O. (2007) Synthesis of glycerol phosphate lipoteichoic acid in Staphylococcus aureus. *Proc. Natl. Acad. Sci. U. S. A.* **104**, 8478–8483
49. Corrigan, R. M., Abbott, J. C., Burhenne, H., Kaever, V., and Gründling, A. (2011) c-di-AMP Is a New Second Messenger in Staphylococcus aureus with a Role in Controlling Cell Size and Envelope Stress. *PLOS Pathog.* **7**, e1002217
50. Upton, C., and Buckley, J. T. (1995) A new family of lipolytic enzymes? *Trends Biochem. Sci.* **20**, 178–179

51. Hopf, T. A., Colwell, L. J., Sheridan, R., Rost, B., Sander, C., and Marks, D. S. (2012) Three-Dimensional Structures of Membrane Proteins from Genomic Sequencing. *Cell*. **149**, 1607–1621